

# Optical conductivity from pair density waves

Zhehao Dai and Patrick A. Lee

*Department of Physics, Massachusetts Institute of Technology, Cambridge, Massachusetts 02139, USA*

(Received 20 September 2016; published 10 January 2017)

We present a theory of optical conductivity in systems with finite-momentum Cooper pairs. In contrast to the BCS pairing where ac conductivity is purely imaginary in the clean limit, there is nonzero ac absorption across the superconducting gap for finite-momentum pairing if we break the Galilean symmetry explicitly in the electronic Hamiltonian. Vertex correction is crucial for maintaining the gauge invariance in the mean-field formalism and dramatically changes the optical conductivity in the direction of the pairing momentum. We carried out a self-consistent calculation and gave an explicit formula for optical conductivity in a simple case. This result applies to the Fulde-Ferrell-Larkin-Ovchinnikov state and candidates with pair density waves proposed for high- $T_c$  cuprates. It may help detect pair density waves and determine the pairing gap as well as the direction of the pairing momentum in experiments.

DOI: [10.1103/PhysRevB.95.014506](https://doi.org/10.1103/PhysRevB.95.014506)

## I. INTRODUCTION

Pair density waves (PDWs) occur when Cooper pairs condense at nonzero momenta. The first example of PDWs is the Fulde-Ferrell-Larkin-Ovchinnikov state (FFLO), where finite-momentum pairing is preferred in a certain range of the Zeeman splitting [1,2]. More recently, experimental evidence of FFLO states has been found in  $\text{CeCoIn}_5$  [3] and  $\kappa$ -(BEDT-TTF) $_2\text{Cu}(\text{NCS})_2$  [BEDT-TTF  $\equiv$  bis(ethylene-dithio)tetrathiafulvalene] [4], and possible mechanisms stabilizing PDWs have been proposed in high- $T_c$  cuprates [5,6]. Unlike conventional BCS superconductors, these phases with PDWs usually have partially gapped Fermi surfaces, almost normal specific heat, and anisotropic electromagnetic response. Although many of the physical properties of PDWs are well established, to the best of our knowledge, the optical conductivity from PDWs has not yet been addressed. The purpose of the present paper is to report the unconventional features in the optical conductivity and to discuss its potential applications in various experimental systems. Most of the results presented here apply to a general class of PDW, but we mainly focus on the case with FFLO pairing where quantitative comparison might be made with experiments in the near future.

It is well known that a single-band BCS superconductor, in the clean limit, has no optical absorption across the superconducting gap [7]. This absence of absorption is not protected by the symmetry of the Hamiltonian but by a special feature of the BCS ground state: single-particle states in the original band carrying opposite currents are always simultaneously occupied (or unoccupied); hence the ground state is an exact eigenstate of the current operator, and the matrix element for ac absorption  $\langle \text{excited state} | \hat{\mathbf{j}} | \text{G.S.} \rangle$  (often called the ‘coherence factor’) vanishes. However, this is not the case for finite-momentum pairing. Although the ground state has zero average current, it is no longer an eigenstate of the current operator. Finite-momentum Cooper pairs are, in general, optically active, and they give rise to the dominant contribution to the ac conductivity in the energy range comparable to the pairing gap.

It is worth mentioning that the ground state generally involves PDWs with multiple pairing momenta if finite-momentum pairing is favorable. For example, if we have Cooper pairs condensing at momentum  $Q$ , it is natural to

have another pairing momentum  $-Q$ . The two pairing terms together cause the folding of the Brillouin zone (BZ), hence charge density waves (CDWs) at momenta  $2Q$ ,  $4Q$ , etc. [2]. It is also possible to have pairing momenta in different directions generating complex incommensurate patterns above the original lattice. However, for simplicity, we focus on the case with only one pairing momentum, a ‘‘pure PDW’’ with no charge modulation. The optical absorption from PDWs with multiple pairing momenta should be qualitatively similar for frequencies around the pairing gap. This pure PDW with only a phase modulation in the pairing order parameter appears to break the lattice translational symmetry, but it is actually invariant under the combination of a gauge transformation and the lattice translation. Note that the absolute phase is not a physical observable, only the phase difference is. Despite the phase modulation, every physical observable in this state is invariant under the lattice translation. In this sense, we do not need to break the translational symmetry further to get new absorption peaks; this is very different from the optical absorption of only CDWs.

One important thing in calculating optical conductivity is maintaining gauge invariance in the self-consistent mean-field approximation. This issue was first discussed in BCS superconductors by Nambu [8] and was recently studied in strongly interacting superconductors [9,10]. The key step is to carry out the vertex correction that is consistent with the gap equation [8–11]. We followed Nambu’s approach and gave an explicit formula for optical conductivity in systems with simple electron-electron interactions. One subtlety in this calculation is that, in order to have nonzero ac conductivity, we must break Galilean symmetry explicitly in the electronic Hamiltonian. This is because the current operator coincides with the momentum operator in a Galilean symmetric system, making the linear response to a uniform electromagnetic field trivial. This issue is discussed in more detail after a brief review of finite-momentum pairing.

## II. FINITE-MOMENTUM PAIRING AND THE GAP EQUATION

We start by briefly reviewing the mean-field treatment of finite-momentum pairing, especially the diagrammatic

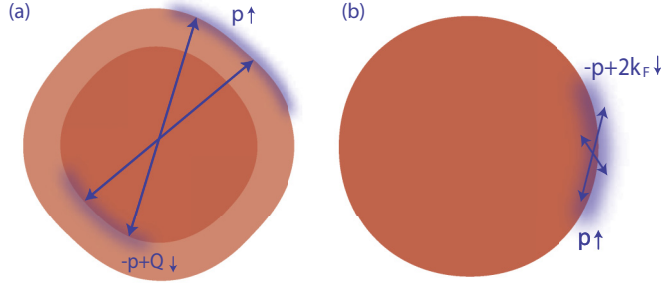


FIG. 1. Two examples of finite-momentum pairing. (a) FFLO pairing. The dark orange region is occupied by both spins, while the light orange region is occupied by only up spin. The blue shaded regions on the Fermi surface are gapped out by pairing. (b) Amperean pairing. A different pairing mechanism without spin splitting, where the vicinity of a hot spot on the Fermi surface is gapped out, and the pairing momentum is close to  $2k_F$ .

interpretation of the mean-field gap equation, which turned out to be useful in calculating linear-response functions.

In the case of FFLO pairing, the Fermi surfaces of up-spin and down-spin electrons are split by Zeeman splitting, but the orbital degree of freedom is not affected. This situation can be realized in layered materials by imposing an in-plane magnetic field. As shown in Fig. 1(a), finite-momentum pairing creates Cooper pairs near the Fermi surfaces and is argued to be more stable than the BCS pairing in a certain range of spin splitting. Another example of finite-momentum pairing is the Amperean pairing shown in Fig. 1(b), where electrons moving in the same direction attract each other by the Lorentz force of the emergent gauge field [6,12].

In the present paper, we consider a (2+1)-dimensional system with Hamiltonian  $H = \sum \epsilon_{p,\sigma} \psi_{p,\sigma}^\dagger \psi_{p,\sigma} + \sum \lambda_k \psi_{p+k,\sigma}^\dagger \psi_{p-k,\sigma'} \psi_{p',\sigma'} \psi_{p,\sigma}$ , where the four-fermion interaction might be mediated by phonon or other more exotic mechanisms. To describe a state with finite-momentum pairing, it is convenient to introduce the two-component Nambu spinor:  $\Psi_p = (\psi_{p+Q/2,\uparrow}, \psi_{-p+Q/2,\downarrow}^\dagger)^T$ , where  $Q$  is the pairing momentum, which should be determined self-consistently to minimize the energy of the mean-field ground state, as shown in Refs. [1,2]. The four-fermion interaction can then be written as  $\sum_{p,p',k} \lambda_k [\Psi_{p+k}^\dagger \tau_3 \Psi_p][\Psi_{p'-k}^\dagger \tau_3 \Psi_{p'}]$ . The mean-field Hamiltonian for finite-momentum pairing is

$$H = \sum_p \Psi_p^\dagger \begin{pmatrix} \epsilon_{p+Q/2,\uparrow} & \Delta_p \\ \Delta_p & -\epsilon_{-p+Q/2,\downarrow} \end{pmatrix} \Psi_p. \quad (1)$$

We would like to point out an important difference from the BCS pairing. In the BCS case, the diagonal terms are always equal with opposite signs, and so are the two eigenvalues. However, this ‘‘particle-hole’’ symmetry is broken in the FFLO state. We may even have an ‘‘unpaired region’’ in the BZ where the two eigenvalues are of the same sign. For convenience, define  $\bar{\epsilon}_p \equiv (\epsilon_{p+Q/2,\uparrow} + \epsilon_{-p+Q/2,\downarrow})/2$ ,  $\epsilon'_p \equiv (\epsilon_{p+Q/2,\uparrow} - \epsilon_{-p+Q/2,\downarrow})/2$ , and  $\delta_p \equiv \sqrt{\bar{\epsilon}_p^2 + \Delta_p^2}$ . The two eigenvalues are given by

$$E_p^\pm = \epsilon'_p \pm \delta_p. \quad (2)$$

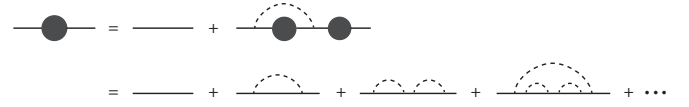


FIG. 2. The self-consistent equation of the mean-field Green’s function and the diagrams included in this approximation. The solid line represents the two-component Nambu spinor, and the dashed line represents the electron-electron interaction mediated by a boson, e.g., phonon. We have ignored the correction of the interaction since it is not important for our purpose. All diagrams without the crossing of the interaction line are included.

The unpaired region is where  $\delta_p < |\epsilon'_p|$ . The boundary of this region where  $\delta_p = |\epsilon'_p|$  is the ‘‘Fermi surface’’ left after FFLO pairing and the shift in momentum. Optical absorption occurs in the ‘‘paired region’’ when the frequency of light matches the splitting between the two bands  $2\delta_p$ .

The Nambu spinor introduced above allows us to treat the pairing gap on an equal footing with the self-energy correction, and the conventional mean-field gap equation can be understood as a Hartree-Fock approximation [8,11]. We approximate the four-fermion interaction by a quadratic term and demand that, to first order, the remaining interaction does not modify the propagator:

$$G(p) = 1/[p_0 - H_0(p) - \Sigma(p) + i \text{sgn}(p_0)0^+], \quad (3)$$

$$0 = -\Sigma(p) + i \int \frac{d^3k}{(2\pi)^3} \lambda_k \tau_3 G(p-k) \tau_3,$$

where  $G(p)$  is the mean-field Green’s function of the Nambu spinor,  $p_0$  is the temporal component of the momentum,  $H_0(p) \equiv \epsilon'_p + \bar{\epsilon}_p \tau_3$  is the Hamiltonian for the original band, and  $\Sigma(p) \equiv \Delta_p \tau_1$  is the pairing term. We have ignored the diagonal self-energy correction in  $\Sigma(p)$  since it is not important for our purpose.

This approximation is equivalent to summing over all Feynman diagrams without crossing in calculating the Green’s function, as shown in Fig. 2.

When the four-fermion interaction has no momentum dependence near the Fermi surface, both  $\lambda_k$  and  $\Delta_p$  can be approximated by constants, and we arrive at the familiar gap equation after integrating out  $k_0$ :

$$\Delta = -\lambda \int_{\text{paired}} \frac{d^2\vec{p}}{(2\pi)^2} \frac{\Delta}{2\sqrt{\bar{\epsilon}_p^2 + \Delta^2}}. \quad (4)$$

This gap equation is almost the same as the BCS gap equation, except the integral is restricted in the paired region.

### III. VERTEX CORRECTION AND GAUGE-INVARIANT ELECTROMAGNETIC RESPONSE

We are now ready to study the electromagnetic response of PDWs. Following the Peierls substitution, we change  $\epsilon_{p,\sigma}$  in the total Hamiltonian into  $\epsilon_{p+eA,\sigma}$ , where  $\vec{A}$  is the magnetic vector potential. We restrict ourselves to the single band near the Fermi level and focus on the limit of a weak and uniform external field as in the case of infrared absorption. Under these

restrictions, the current operator  $\vec{j} \equiv -\partial H/\partial \vec{A}$  can be written as

$$\vec{j} = \sum_{p,\sigma} \psi_{p,\sigma}^\dagger [-e\vec{v}_{p,\sigma} - e^2 \mathbf{m}_p^{-1} \vec{A}] \psi_{p,\sigma} \quad (5)$$

$$\equiv \sum_p \Psi_p^\dagger [-e\vec{v}_1(\vec{p})\mathbb{1} - e\vec{v}_2(\vec{p})\tau_3 - e^2 \mathbb{m}_p^{-1} \vec{A}] \Psi_p, \quad (6)$$

where  $\vec{v}_{p,\sigma} \equiv \nabla_p \epsilon_{p,\sigma}$  is the band velocity and  $\mathbf{m}_p \equiv (\nabla_p \nabla_p \epsilon_{p,\sigma})^{-1}$  is the effective-mass tensor.  $\vec{v}_1(\vec{p})$ ,  $\vec{v}_2(\vec{p})$ , and  $\mathbb{m}_p$  are defined by the equation above, and they depend on the pairing momentum. The current operator at zero field is usually called the paramagnetic current, and we would like to write the spatial components together with the temporal component  $j_0 = \sum_{p,\sigma} -e\psi_{p,\sigma}^\dagger \psi_{p,\sigma}$  as

$$j_\mu^P = \sum_p \Psi_p^\dagger \gamma_\mu(\vec{p}) \Psi_p, \quad (7)$$

$$\gamma_\mu(\vec{p}) \equiv -e(\tau_3, \vec{v}_1(\vec{p})\mathbb{1} + \vec{v}_2(\vec{p})\tau_3). \quad (8)$$

The part of the current proportional to  $\vec{A}$  in Eqs. (5) and (6) is called the diamagnetic current, which does not contribute to the real part of the conductivity at any finite frequency.

Naively, one would like to plug the paramagnetic current and the mean-field excited states into the Kubo formula:

$$\text{Re } \sigma_{ii} = \frac{\pi}{\omega} \sum_n |\langle 0 | j_i^P | n \rangle|^2 \delta(\omega - E_n + E_0), \quad (9)$$

where  $i$  denotes the spatial components and 0 ( $n$ ) denotes the ground state (excited states). This approach corresponds to plugging the mean-field Green's function into the bubble diagram without doing other corrections.

As explained in the Introduction, the matrix element  $\langle 0 | j_i^P | n \rangle$  vanishes identically for BCS pairing but not for finite-momentum pairing. Thus we expect a nonzero ac conductivity for a state with PDWs. However, the bare result given by the “mean-field version” of Eq. (9) cannot be trusted for at least two reasons: (1) This approach violates gauge invariance, specifically the Ward-Takahashi identity between the vertex and the Green's function [8,11]. (2) The result given by Eq. (9) is always nonzero for any finite-momentum pairing, but the ac conductivity should be exactly zero if the electronic Hamiltonian is Galilean invariant.

The latter statement may not be immediately obvious, especially in the case with spontaneous symmetry breaking. So we give a careful explanation in this paragraph. When the energy band is parabolic, the current operator is proportional to the kinetic momentum operator:  $(\vec{j}(t)) = -e(\vec{P}(t))/m - ne^2 \vec{A}(t)/m$ , where  $\vec{P}$  is the canonical momentum per unit volume. Since  $\vec{P}$  commutes with the Hamiltonian under uniform perturbation, its average value remains zero all the time. Thus the linear response is trivial, and we get  $\sigma(\omega) = ie^2 n/m(\omega + i0^+)$ . We can see that there is only a  $\delta$  function in the real part of the conductivity, and this derivation holds regardless of whether the ground state is a symmetry-breaking state or not.

The inconsistencies (1) and (2) can be solved by a well-known technique in QED, first introduced to superconductors by Nambu to restore the gauge invariance in the BCS formalism [8,11,13]. The key observation is that, whenever

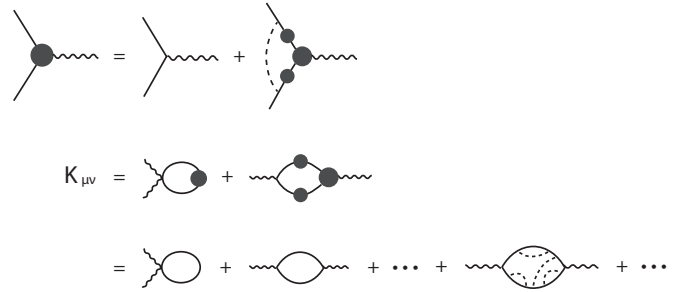


FIG. 3. The self-consistent vertex correction and the diagrams included in the corrected electromagnetic response function  $K_{\mu\nu}$  (defined as  $j_\mu = K_{\mu\nu} A_\nu$ ). The solid line represents the Nambu spinor, the dashed line represents the electron-electron interaction, and the wavy line represents the electromagnetic field. The second diagram on the first line of  $K_{\mu\nu}$  is the paramagnetic response  $P_{\mu\nu}$ .

an electron-photon vertex appears in a chain of electron lines, we can always form a “gauge-invariant subgroup” of diagrams by considering all different places to insert the corresponding photon line along this chain. The Ward-Takahashi identity is automatically preserved if we sum over all diagrams in this subgroup. As discussed in the previous section, the mean-field Green's function contains all diagrams without crossing. Following the diagrammatic technique, if we plug the mean-field Green's function into the bubble diagram, we are forced to include all corrections to the bubble diagram without crossing. This can be done by introducing a corrected electron-photon vertex, as shown in Fig. 3. Those diagrams containing a two-electron-two-photon vertex correspond to the average value of the diamagnetic current, which does not contribute to the imaginary part of the response function (real part of the conductivity) at any finite frequency, so we focus on the paramagnetic part of the response function (defined as  $j_\mu^P = P_{\mu\nu} A_\nu$ ):

$$P_{\mu\nu} = -i \int \frac{d^3 p}{(2\pi)^3} \text{Tr}[\gamma_\mu(p, p') G_{p'} \Gamma_\nu(p', p) G_p], \quad (10)$$

where  $\gamma_\mu(p, p')$  [ $\Gamma_\mu(p, p')$ ] is the bare (corrected) vertex of the two-electron-one-photon interaction.  $\Gamma_\mu(p, p')$  is given by a self-consistent equation as depicted in Fig. 3:

$$\Gamma_\mu(p', p) = \gamma_\mu(p', p) + i \int \frac{d^3 k}{(2\pi)^3} \lambda_k \tau_3 G(p' - k) \times \Gamma_\mu(p' - k, p - k) G(p - k) \tau_3. \quad (11)$$

We are interested in the case  $\vec{p} = \vec{p}'$ , and we have  $\gamma_\mu([p_0 + \omega, \vec{p}], [p_0, \vec{p}]) = \gamma_\mu(\vec{p})$ , as shown in Eqs. (7) and (8).

Equation (11) can be solved analytically when the four-fermion interaction has no momentum dependence near the Fermi surface. If we further assume the pairing gap  $\Delta$  is much smaller than the bandwidth, the self-consistent vertex acquires a simple form:

$$\vec{\Gamma} = -e[\vec{v}_1(\vec{p})\mathbb{1} + \vec{v}_2(\vec{p})\tau_3 + 2i\Delta I(\vec{v}_2)\tau_2/\omega I(1)], \quad (12)$$

$$I(f) \equiv \int_{\text{paired}} \frac{d^2 \vec{p}}{(2\pi)^2} \frac{f(p)}{\delta_p(\omega - 2\delta_p)(\omega + 2\delta_p)}, \quad (13)$$

where  $I(f)$  is a linear functional defined by the integral which appears repeatedly in the remaining part of the paper. Finally, the corrected optical conductivity is given by

$$\text{Re}\sigma_{ij}(\omega > 0) = -\text{Im} P_{ij}(\omega > 0)/\omega \quad (14)$$

$$= -\frac{4e^2\Delta^2}{\hbar\omega} \text{Im}[I(v_{2i}v_{2j}) - I(v_{2i})I(v_{2j})/I(1)]. \quad (15)$$

Note that we have omitted the infinitesimal imaginary part of  $\omega$  in the integral (13) since the pole structure in retarded response functions is different from that in path integrals, and  $\omega$  should always be replaced by  $\omega + i0^+$  for the retarded response. When  $\omega > 0$ , the imaginary part of the integral is given by

$$\text{Im} I(f) = -\pi \int_{\text{paired}} \frac{d^2\vec{p}}{(2\pi)^2} \frac{f(p)}{4\delta_p^2} \delta(\omega - 2\delta_p), \quad (16)$$

which is proportional to the joint density of states (JDOS) in the paired region. We found that the first term in Eq. (15) is nothing but the bare result given by the mean-field version of Eq. (9), while the second term is given by the vertex correction. As discussed before, only those points in the paired region of the BZ where the frequency matches the band splitting contribute to the real part of the optical conductivity. For a given  $\omega$ , these points lie on arcs in the BZ.

Another important ingredient in Eq. (15) is  $\vec{v}_2$ . Recall that  $\vec{v}_2$  is defined by Eqs. (5) and (6). In the case of FFLO pairing, when the pairing momentum is much smaller than the Fermi momentum, we have

$$v_{2i}(\vec{p}) = (\mathbf{m}_p^{-1})_{ij} Q_j/2 + O(Q^2). \quad (17)$$

As discussed above, gauge invariance is guaranteed in this formalism. Furthermore, we found that the problem regarding Galilean symmetry is automatically solved: if the band is parabolic,  $\vec{v}_2 = \mathbf{Q}/2m = \text{const}$ ; hence  $v_{2i}$  and  $v_{2j}$  can be dragged out of the integral in Eq. (15), and the vertex correction cancels the bare result. However, there is no exact Galilean symmetry in real solids, and Eqs. (15) and (17) show that the optical conductivity from PDWs is proportional to  $Q^2$ . We refer the readers to the Appendix for more details on the Ward-Takahashi identity, the vertex correction, and the final result for optical conductivity.

#### IV. RESULTS FOR TIGHT-BINDING BANDS

We have calculated the optical conductivity of FFLO states explicitly for tight-binding bands with nearest-neighbor (NN) hopping  $t_1$  and next-nearest-neighbor (NNN) hopping  $t_2$  on a square lattice. The result shown in Fig. 4 is for  $t_2/t_1 = 0.35$ , spin splitting  $0.4t_1$ , at half filling. The pairing momentum is  $(0.1/a, 0.1/a)$ , where  $a$  is the lattice constant. The ac conductivity shows up in both Figs. 4(a) and 4(b) above  $2\Delta$ , and there are divergent peaks right at  $2\Delta$  [although the divergence of the blue curve in Fig. 4(a) appears to be small, it is guaranteed to be a true divergence by analytical analysis of Eq. (15)] due to the corresponding divergence in the JDOS. As mentioned in the previous section, for a given  $\omega$ , only the arcs in the BZ satisfying the frequency-matching condition contribute to ac absorption. When  $\delta\omega \equiv \omega - 2\Delta \simeq 0$ , the frequency-matching

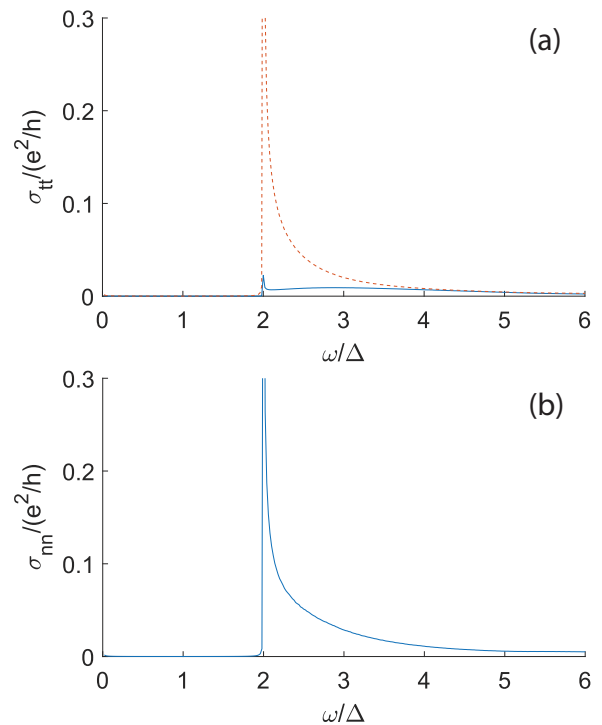


FIG. 4. Optical conductivity of the FFLO state calculated for tight-binding bands on a two-dimensional square lattice,  $t_2/t_1 = 0.35$ . The spin splitting is set to be  $0.4t_1$ , which is about 4% of the bandwidth, and the pairing momentum is  $(0.1/a, 0.1/a)$ . (a) Conductivity in the direction of the pairing momentum. The dashed orange line is the bare result, and the blue line is the corrected result. (b) Conductivity in the perpendicular direction. The vertex correction is identically zero in this direction by symmetry.

condition  $\omega = 2\delta_p$  gives  $\vec{\epsilon}_p = \sqrt{\omega^2/4 - \Delta^2} \propto \sqrt{\delta\omega}$ ; then the JDOS is  $N(0)d\vec{\epsilon}_p/d\omega \propto 1/\sqrt{\delta\omega}$ , where  $N(0)$  is the density of states (DOS) of the normal metal. Hence the  $1/\sqrt{\delta\omega}$  divergence in the optical conductivity at  $2\Delta$ . This divergence has the same form as the divergence in the DOS and JDOS of  $s$ -wave BCS superconductors, but the real part of the ac conductivity is identically zero in BCS superconductors for any band structure, as explained in the Introduction.

The effects of the vertex correction on divergent peaks depend on the type of divergence as well as the details of the band structure and can be dramatically different in different situations. If there is a single singularity of the JDOS on the frequency-matching arc giving the dominant contribution, we can replace  $\vec{v}_2$  by its value at the singularity, and it is clear from Eq. (15) that the vertex correction completely cancels the divergence in the bare result. However, the divergence at  $2\Delta$  is due to the whole arc in the paired region satisfying  $\vec{\epsilon}_p \simeq 0$ , and it remains divergent after the vertex correction. The ratio between the corrected result [shown as a blue line in Fig. 4(a)] and the bare result [dashed orange line in Fig. 4(a)] depends on the variance of  $\vec{v}_2$  on the frequency-matching arc. We found that in the current example, the divergence in the conductivity along the pairing momentum  $\sigma_{\parallel}$  is strongly suppressed by the vertex correction, whereas there is no vertex correction at all in the perpendicular direction since the perpendicular component of  $\vec{v}_2$  is odd under the reflection over  $(\pi, \pi)$ .

## V. DISCUSSION

We have shown that there is nonzero ac absorption from PDWs if we break Galilean symmetry explicitly in the electronic Hamiltonian (which is usually the case in solids). When the pairing momentum  $Q$  is much smaller than the Fermi momentum  $p_F$  and the pairing gap  $\Delta$  is much smaller than the bandwidth  $W$ , the ac conductivity is proportional to  $(Q/p_F)^2 W/\Delta$ . We estimated the typical optical conductivity in  $\kappa$ -(BEDT-TTF)<sub>2</sub>Cu(NCS)<sub>2</sub> around the frequency of the pairing gap and away from the divergent peak to be on the order of  $0.01e^2/h$  based on the recent experiment [4]. However, since a direct measure of the pairing momentum and the pairing gap is still missing, it is hard to give a more accurate estimation. Vertex correction plays an important role in this ac absorption and dramatically changes the behavior of the optical conductivity in the direction of the pairing momentum.

This nonzero absorption could be used as experimental evidence for PDWs. Furthermore, the various features discussed in the previous section can help determine the pairing gap and the direction of the pairing momentum in experiments. We have focused on the case with only one pairing momentum in the present paper, and we have ignored the momentum dependence of the pairing gap near the Fermi surface in the explicit calculation. The results for more general PDWs should be similar, but we would like to discuss some possible differences in this paragraph. (1) A weak momentum dependence of the pairing gap introduces a cutoff to the  $1/\sqrt{\delta\omega}$  divergence at  $\omega = 2 \min[\Delta_p]$ , whereas a strong momentum dependence completely destroys the  $1/\sqrt{\delta\omega}$  behavior and leaves only a finite jump. (2) When the PDW state has more than one pairing momentum, one or more CDWs will be generated by the interference, and there will be nonzero absorption below the “pairing gap”  $2 \min[\Delta_p]$ . The magnitude of this “in-gap” absorption increases with the magnitude of the CDW. (3) We have not discussed the effect of impurities so far. Since there is a finite density of states left at Fermi level, there will be a Drude peak coexisting with the absorption we discussed when the inverse of the mean free time of electrons is smaller than the pairing gap. However, in the opposite limit, even BCS superconductors have nonzero optical absorption above the gap [7], and there is no sharp feature for PDWs.

## ACKNOWLEDGMENT

P.A.L. acknowledges support from the NSF under Grant No. DMR-1522575.

## APPENDIX

We present the derivation of Eqs. (12) and (15) in this appendix. For simplicity, we define  $\tilde{p}_0 \equiv p_0 - \epsilon'_p$ . The Green's function given by Eq. (3) can then be written as

$$G(p) = \frac{1}{\tilde{p}_0 - \bar{\epsilon}_p \tau_3 - \Delta_p \tau_1 + i \text{sgn}(p_0) 0^+} = \frac{\tilde{p}_0 + \bar{\epsilon}_p \tau_3 + \Delta_p \tau_1}{[\tilde{p}_0 + i \text{sgn}(p_0) 0^+]^2 - \delta_p^2}, \quad (\text{A1})$$

where we have neglected the diagonal self-energy correction since it is not important for our purpose. We are free to choose the “direction” of the pairing term in the  $\tau_1 - \tau_2$  plane since they are related by gauge symmetry. The temporal component of the self-consistent vertex  $\Gamma_t$  in the limit  $|\vec{q}| \rightarrow 0$  ( $q$  is the momentum of the external field) is determined directly by the Ward-Takahashi identity,

$$q_\mu \Gamma_\mu(p+q, p) = -e\tau_3 G^{-1}(p) + eG^{-1}(p+q)\tau_3, \quad (\text{A2})$$

where  $q_\mu \Gamma_\mu$  is shorthand for  $\vec{q} \cdot \vec{\Gamma} - \omega \Gamma_t$ . Note that there are additional  $\tau_3$  compared to the standard Ward-Takahashi identity in QED since the two components of the Nambu spinor carry opposite charges. If we assume the spatial components of  $\Gamma$  do not diverge in the limit  $|\vec{q}| \rightarrow 0$ , which can be verified later, only the temporal component of  $\Gamma$  contributes the left-hand side, and we have

$$\begin{aligned} \Gamma_t([p_0 + \omega, \vec{p}], [p_0, \vec{p}]) &= -[-e\tau_3 G^{-1}(p) + eG^{-1}(p+q)\tau_3]/\omega \\ &= -e(\tau_3 + 2i\Delta_p \tau_2/\omega). \end{aligned} \quad (\text{A3})$$

On the other hand, the spatial components of  $\Gamma$  take some calculation, and they acquire a simple form only when the four-fermion interaction has no momentum dependence near the Fermi surface. In this case  $\lambda_k$  can be treated as a constant, and the self-consistent equation [Eq. (3)] shows that  $\Delta_p$  is also a constant near the Fermi surface. Plugging the mean-field Green's function into Eq. (11) and shifting the momentum of the integration, we have

$$\Gamma_\mu([p_0 + \omega, \vec{p}], [p_0, \vec{p}]) = \gamma_\mu(\vec{p}) + i\lambda \int \frac{d^3 p}{(2\pi)^3} \frac{\tau_3(\tilde{p}_0 + \omega + \bar{\epsilon}_p \tau_3 + \Delta_p \tau_1) \Gamma_\mu([p_0 + \omega, \vec{p}], [p_0, \vec{p}]) (\tilde{p}_0 + \bar{\epsilon}_p \tau_3 + \Delta_p \tau_1) \tau_3}{\{[\tilde{p}_0 + \omega + i \text{sgn}(p_0 + \omega) 0^+]^2 - \delta_p^2\} \{[\tilde{p}_0 + i \text{sgn}(p_0) 0^+]^2 - \delta_p^2\}}. \quad (\text{A4})$$

It is clear from the equation above that the vertex correction has no  $p$  dependence; this is, of course, true only when we ignore the momentum dependence of the four-fermion interaction. In this case, we can write the self-consistent vertex as

$$\Gamma_\mu([p_0 + \omega, \vec{p}], [p_0, \vec{p}]) = \gamma_\mu(\vec{p}) - e\Gamma_\mu^0 \mathbb{1} - e \sum_{i=1}^3 \Gamma_\mu^i \tau_i, \quad (\text{A5})$$

where  $\Gamma^0$  and  $\Gamma^i$  are functions of  $\omega$  and  $\gamma_\mu(\vec{p})$  is given by Eqs. (7) and (8). The next step is to plug Eq. (A5) into

Eq. (A4), compute the matrix multiplication in the numerator, carry out the integral of  $p_0$  using the residue theorem, and solve  $\Gamma^0$  and  $\Gamma^i$ . Note that there are four poles of  $p_0$  in the complex plane, whose imaginary parts depend on the spatial momentum  $\vec{p}$ . If  $\vec{p}$  lies in the unpaired region, the two eigenenergies  $E_p^\pm$  are of the same sign, so the four poles locate on the same side of the real axis. Then we know the integral must be zero since we can complete the contour on the other side including none of the residues. This observation confirms our statement that only the paired region in the

BZ contributes to the optical conductivity. After all these laborious calculations, we arrive at the self-consistent equation for  $\vec{\Gamma}^0$  and  $\vec{\Gamma}^i$  (the spatial components of  $\Gamma^0$  and  $\Gamma^i$ ). We

show that, by direct calculation, the integral in Eq. (A4) has no identity component; thus  $\vec{\Gamma}^0 = 0$ . On the other hand,  $\vec{\Gamma}^i$  satisfies

$$\begin{pmatrix} \vec{\Gamma}^1 \\ \vec{\Gamma}^2 \\ \vec{\Gamma}^3 \end{pmatrix} = \lambda \begin{pmatrix} 2I(\bar{\epsilon}_p^2) & -i\omega I(\bar{\epsilon}_p) & -2\Delta I(\bar{\epsilon}_p) \\ i\omega I(\bar{\epsilon}_p) & 2I(\delta_p^2) & -i\omega\Delta I(1) \\ 2\Delta I(\bar{\epsilon}_p) & -i\omega\Delta I(1) & -2\Delta^2 I(1) \end{pmatrix} \begin{pmatrix} \vec{\Gamma}^1 \\ \vec{\Gamma}^2 \\ \vec{\Gamma}^3 \end{pmatrix} + \lambda \begin{pmatrix} -2\Delta I(\bar{\epsilon}_p \vec{v}_2) \\ -i\omega\Delta I(\vec{v}_2) \\ -2\Delta^2 I(\vec{v}_2) \end{pmatrix}, \quad (\text{A6})$$

where

$$I(f(\vec{p})) \equiv \int_{\text{paired}} \frac{d^2\vec{p}}{(2\pi)^2} \frac{f(p)}{\delta_p[\omega - 2\delta_p + i\text{sgn}(\omega)0^+][\omega + 2\delta_p + i\text{sgn}(\omega)0^+]}. \quad (\text{A7})$$

If we further assume the pairing gap  $\Delta$  and the frequency  $\omega$  are much smaller than the bandwidth, only a thin shell near  $\bar{\epsilon}_p = 0$  contributes to the integral. In this limit  $I(\bar{\epsilon}_p) \sim 0$ ,  $I(\bar{\epsilon}_p \vec{v}_2) \sim 0$ , so we have  $\vec{\Gamma}^1 \sim 0$ , and  $\vec{\Gamma}^2$  and  $\vec{\Gamma}^3$  satisfy

$$\begin{pmatrix} \vec{\Gamma}^2 \\ \vec{\Gamma}^3 \end{pmatrix} = \lambda \begin{pmatrix} 2I(\delta_p^2) & -i\omega\Delta I(1) \\ -i\omega\Delta I(1) & -2\Delta^2 I(1) \end{pmatrix} \begin{pmatrix} \vec{\Gamma}^2 \\ \vec{\Gamma}^3 \end{pmatrix} - \lambda I(\vec{v}_2) \begin{pmatrix} i\omega\Delta \\ 2\Delta^2 \end{pmatrix}. \quad (\text{A8})$$

In addition, the mean-field gap equation [Eq. (4)] gives us

$$\begin{aligned} 4\lambda I(\delta_p^2) - \lambda\omega^2 I(1) &= -\lambda I(\omega^2 - 4\delta_p^2) \\ &= -2\lambda \int_{\text{paired}} \frac{d^2\vec{p}}{(2\pi)^2} \frac{1}{2\sqrt{\bar{\epsilon}_p^2 + \Delta^2}} = 2. \end{aligned} \quad (\text{A9})$$

Using this identity, we can easily find

$$\vec{\Gamma}^2 = \frac{2i\Delta I(\vec{v}_2)}{\omega I(1)}, \quad \vec{\Gamma}^3 = 0. \quad (\text{A10})$$

So the corrected vertex is

$$\begin{aligned} \Gamma_\mu([p_0 + \omega, \vec{p}], [p_0, \vec{p}]) &= -e[\tau_3 + 2i\Delta\tau_2/\omega, \vec{v}_1(\vec{p})\mathbb{1} \\ &\quad + \vec{v}_2(\vec{p})\tau_3 + 2i\Delta I(\vec{v}_2)\tau_2/\omega I(1)]. \end{aligned} \quad (\text{A11})$$

We are now ready to calculate the paramagnetic response function  $P_{\mu\nu}$ . For simplicity, define

$$\langle f, h \rangle \equiv -i \int \frac{d^3p}{(2\pi)^3} \text{Tr}[f(p, p')G_{p'}h(p', p)G_p]. \quad (\text{A12})$$

Then we have

$$P_{ij} = \langle \gamma_i, \Gamma_j \rangle \quad (\text{A13})$$

$$\begin{aligned} &= e^2 \langle v_{1i}(\vec{p})\mathbb{1} + v_{2i}(\vec{p})\tau_3, v_{1j}(\vec{p})\mathbb{1} + v_{2j}(\vec{p})\tau_3 \\ &\quad + 2i\Delta I(v_{2j})\tau_2/\omega I(1) \end{aligned} \quad (\text{A14})$$

$$\begin{aligned} &= e^2 \langle v_{2i}(\vec{p})\tau_3, v_{2j}(\vec{p})\tau_3 \rangle + [2i\Delta I(v_{2j})/\omega I(1)] \\ &\quad \times e^2 \langle v_{2i}(\vec{p})\tau_3, \tau_2 \rangle, \end{aligned} \quad (\text{A15})$$

where we have used the fact that the identity component of the vertex does not contribute to the integral, which can be verified explicitly. Integrating out  $p_0$ , we have

$$P_{ij} = 4e^2\Delta^2[I(v_{2i}v_{2j}) - I(v_{2i})I(v_{2j})/I(1)]. \quad (\text{A16})$$

This result leads to the result for optical conductivity in Eq. (15). We would like to remind the readers again that Eq. (15) holds only for  $\omega > 0$  if we define the integral  $I(f(\vec{p}))$  as in Eq. (A7); this is due to the difference between the path integral and retarded response. It holds for both positive and negative  $\omega$  if we replace the infinitesimal imaginary part  $i\text{sgn}(\omega)0^+$  in the integral  $I(f(\vec{p}))$  by  $i0^+$ .

- [1] P. Fulde and R. A. Ferrell, *Phys. Rev.* **135**, A550 (1964).
- [2] A. I. Larkin and Y. N. Ovchinnikov, *Sov. Phys. JETP* **20**, 762 (1965).
- [3] A. Bianchi, R. Movshovich, C. Capan, P. G. Pagliuso, and J. L. Sarrao, *Phys. Rev. Lett.* **91**, 187004 (2003).
- [4] H. Mayaffre, S. Krämer, M. Horvatić, C. Berthier, K. Miyagawa, K. Kanoda, and V. Mitrović, *Nat. Phys.* **10**, 928 (2014).
- [5] E. Berg, E. Fradkin, S. A. Kivelson, and J. M. Tranquada, *New J. Phys.* **11**, 115004 (2009).
- [6] P. A. Lee, *Phys. Rev. X* **4**, 031017 (2014).
- [7] G. D. Mahan, *Many-Particle Physics* (Springer, Berlin, 2013).

- [8] Y. Nambu, *Phys. Rev.* **117**, 648 (1960).
- [9] Y. He and H. Guo, [arXiv:1505.04080](https://arxiv.org/abs/1505.04080).
- [10] R. Boyack, B. M. Anderson, C.-T. Wu, and K. Levin, *Phys. Rev. B* **94**, 094508 (2016).
- [11] J. Schrieffer, *Theory of Superconductivity* (Benjamin, New York, 1964).
- [12] S.-S. Lee, P. A. Lee, and T. Senthil, *Phys. Rev. Lett.* **98**, 067006 (2007).
- [13] M. Peskin and D. Schroeder, *An Introduction to Quantum Field Theory*, Advanced Book Classics (Addison-Wesley, Reading, MA, 1995).